HHS Public Access

Author manuscript

Dent Mater. Author manuscript; available in PMC 2019 January 01.

Published in final edited form as:

Dent Mater. 2018 January ; 34(1): e8–e14. doi:10.1016/j.dental.2017.11.004.

Using glass-graded zirconia to increase delamination growth resistance in porcelain/zirconia dental structures

Herzl Chai[1], **Adam J. Mieleszko**[2], **Stephen J. Chu**[2,3], and **Yu Zhang**[4]

[1]Tel Aviv University, School of Mechanical Engineering, Faculty of Engineering, Tel Aviv, Israel

[2]Synergistic Dentistry of New York, 150 East 58th Street, Suite 3200, New York, NY 10155, USA

[3]New York University College of Dentistry, Department of Periodontology & Implant Dentistry and Department of Prosthodontics, 345 E. 24th Street, New York, NY 10010, USA

[4]New York University College of Dentistry, Department of Biomaterials and Biomimetics, 433 First Avenue, Room 810, New York, NY 10010, USA

Abstract

Objective—Porcelain fused to zirconia (PFZ) restorations are widely used in prosthetic dentistry. However, their tendency to delaminate along the P/Z interface remains a practical problem so that assessing and improving the interfacial strength are important design aspects. This work examines the effect of modifying the zirconia veneering surface with an in-house felspathic glass on the interfacial fracture resistance of fused P/Z.

Methods—Three material systems are studied: porcelain fused to zirconia (control) and porcelain fused to glass-graded zirconia with and without the presence of a glass interlayer. The specimens were loaded in a four-point-bend fixture with the porcelain veneer in tension. The evolution of damage is followed with the aid of a video camera. The interfacial fracture energy G_C was determined with the aid of a FEA, taking into account the stress shielding effects due to the presence of adjacent channel cracks.

Results—Similarly to a previous study on PFZ specimens, the fracture sequence consisted of unstable growth of channel cracks in the veneer followed by stable cracking along the P/Z interface. However, the value of G_C for the graded zirconia was approximately 3 times that of the control zirconia, which is due to the good adhesion between porcelain and the glass network structure on the zirconia surface.

Significance—Combined with its improved bonding to resin-based cements, increased resistance to surface damage and good esthetic quality, graded zirconia emerges as a viable material concept for dental restorations.

Corresponding author: Prof. Yu Zhang, Department of Biomaterials and Biomimetics, New York University College of Dentistry, 433 First Avenue, Room 810, New York, NY 10010, USA, Tel.: +1-212-998-9637, yz21@nyu.edu.

Disclosure

All authors declare no conflict of interest.

Keywords

all-ceramic dental restorations; porcelain fused to zirconia; porcelain-veneered graded zirconia; interfacial fracture energy

1. Introduction

Porcelain (veneer) fused to zirconia (PFZ) is commonly used in crowns and fixed dental prostheses (FDPs). However, as demonstrated in numerous clinical research [1–4] and laboratory fatigue studies [5–7] of PFZ restorations, delamination between porcelain and zirconia may become a detrimental factor once occlusal cracks grow all the way to the porcelain/zirconia (P/Z) interface. In general, when cracks in the porcelain veneer reach the veneer/core interface, they tend to graze along the interface before deflecting back into the porcelain veneer rather than penetrate the stiffer and tougher zirconia core [4,7]. This type of failure is motivated by the low interfacial fracture energy G_C of PFZ [8,9] as well as presence of deleterious residual tensile stresses, formed during the veneer firing or glaze firing process due to mismatch in thermal expansion coefficients between veneer and core and low thermal diffusivities characterizing both porcelain and zirconia [10–16]. The weak delamination resistance of the P/Z interface is generally attributed to the chemical inertness of the zirconia phase. Attempts at modifying the surface of the latter by techniques such as grit blasting or the use of an intermittent glass bonding layer between zirconia and porcelain generally yield only marginal improvement. More recently, a good improvement in shear bond strength was reported due to the application of a composite interlayer between porcelain and a zirconia substrate containing surface holes [17].

A promising concept for enhancing mechanical properties of dental restoration is the use of glass-ceramic infiltration techniques to produce functionally graded glass-zirconia materials [18]. A recent application of this approach to the bonding between resin-based dental cements and zirconia led to a considerable increase in the Mode I interfacial fracture energy [19]. This benefit, maintained under stringent testing program including thermal cyclic stressing, was due to the better adhesion between composite cement and the interconnected glass network in the graded zirconia surface. On the other hand, grit blasting of the zirconia bonding surface was of little consequence. Accordingly, in this work we explore the use of the graded zirconia approach for improving the fracture resistance of the P/Z interface.

Assessing interfacial strength of porcelain-veneered zirconia restorations is often done by subjecting the structure to some form of external forces and examining the ensuing fracture pattern [20–23]. While useful for routine material screening, the results are often marred by large experimental scatter reflecting sensitivity to flaws, geometric misalignments of the test specimen and loading fixture, and uneven stress distribution at the interface. These difficulties may be circumvented using Fracture Mechanics concepts, which involve the recording of crack lengths and associated load levels. The results are expressed in terms of fracture energy (per unit area) G_C. A popular test specimen for assessing interfacial strength is the four-point-bending (FPB) bilayer [24]. This specimen was used to determine interfacial fracture energy of porcelain fused to zirconia [8] or metal [9,25] copings. More

recently, the FPB specimen was applied to glass/polymer [26] and PFZ [27] combinations where the evolution of damage was observed *in situ* using a high-power zoom lens. As demonstrated in Fig. 1, this approach revealed an interesting sequence of fracture events involving the growth of multiple channel cracks in the veneering layer, initiation of delamination from the tips of channel cracks, and stable growth of ensuing cracks along the veneer/core interface. A Finite Element Analysis (FEA) of the fracture behavior showed that the presence of channel cracks greatly alter the delamination growth behavior and in turn the calculation of G_C [26,27]. In this study we examine the merit of using the glass-graded zirconia approach for improving fracture resistance in fused P/Z interfaces. The tests and data reduction schemes are much similar to those used in a previous study on unmodified PFZ systems [27].

2. Materials and methods

2.1. Specimen preparation

Three different material groups are used: porcelain fused to zirconia (PFZ), graded zirconia (PFGZ) and graded zirconia in the presence of glass interlayer (PFGGZ). Prior to veneering, the zirconia (Y-TZP, Tosoh TZ-3Y-E grade, CTE = 10.5×10^{-6} K^{-1}) surface was sandblasted with 50 μm Al_2O_3 particles for 5 s at a standoff distance of 10 mm and a compressed air pressure of 2 bars. The graded Y-TZP was prepared as described earlier [18]. Briefly, an in-house prepared glass with composition similar to dental porcelain in the form of powder slurry was first applied on pre-sintered Y-TZP (1350 °C for 1 hour). Glass infiltration and densification occurred in a single process at 1450 °C for 2 hours. This produced a structure consisted of a ~30 μm thick outer surface residual glass layer followed by a ~120 μm thick graded glass-zirconia layer where the content of intergranular glass gradually diminishes and finally transitions into a dense Y-TZP interior [18]. The glass-infiltrated zirconia bars were randomly divided into 2 groups. For the PFGGZ group, the surface residual glass was lightly polished with 6 μm diamond grits. For the PFGZ group, the surface residual glass layer was gently removed by polishing, again using 6 μm diamond grits, to expose the graded glass-zirconia layer. Prior to veneering, the recipient surface of the PFGZ and PFGGZ groups were etched with 4% hydrofluoric acid for 5 mins, water rinsed and dried. A commercially available porcelain powder (Heraceram Zirconia, leucite-reinforced porcelain, CTE = 10.5×10^{-6} K^{-1}, Heraeus Kulzer GmbH, Hanau, Germany) was used to veneer all specimen groups and the firing temperature was 870 °C with a dwell time of 1 min. Examination of the interface zone in the PFGGZ group with optical microscope revealed no visible sign of the interlaminar glass layer, indicating good inter-diffusion between the residual glass and porcelain.

Figure 1 shows a PFZ specimen in its loading fixture. All specimens were fabricated in the desired form: length L = 30 mm, total thickness H = 3.5 mm and width b = 2.5 mm. The porcelain layer thickness h varied in the range 0.40 – 0.55 mm; the use of variable h is beneficial in increasing the testing range and in turn confidence in the calculated G_C. Ten specimens were prepared for each group. Prior to testing, the tensile surface of porcelain was polished down to a 1 μm diamond suspension finish. The distances between lower and upper supporting pins, l and d, were 20 and 10 mm, respectively. The specimens were loaded in a

standard universal testing machine at a rate of 0.1 mm/min. One specimen side face, polished to mirror surface quality, was observed during the loading by a video camera (Canon EOS-5D) equipped with a high-power zoom lens (Optem, Inc.). From these records crack lengths and corresponding load values could be extracted.

2.2. Analysis

Figure 1 shows the fracture model used for calculating the interfacial fracture energy G_C. The specimens are loaded by axial force P which produces bending moment $M = P(l - d)/4$ in the beam portion bounded by the upper supporting pins. The fracture pattern consists of an array of channel cracks in porcelain spaced a fixed distance s apart and interface cracks of length c that emanate symmetrically from each tip of the channel cracks. The energy release rate (ERR) associated with delamination growth along the veneer/core interface was determined by a 2D FEA taking into account the presence of channel cracks [27]. The result is given as

$$G=G^{SS}f(c/s),\ f=1-1.5e^{-0.37s/c} \quad (1a)$$

$$G^{SS}\equiv 1.5(1-\nu_z{}^2)[P(l-d)/2b]^2(E_zH^3)^{-1}[(1-\underline{h})^{-3}-\gamma/Q] \quad (1b)$$

$$Q\equiv \underline{h}^3+\gamma(1-\underline{h})^3+3[\underline{h}^{-1}+\gamma(1-\underline{h})^{-1}]^{-1},\gamma\equiv(1-\nu_p{}^2)/\underline{E}(1-\nu_z{}^2) \quad (1c)$$

$$\underline{E}\equiv E_p/E_z,\underline{h}\equiv h/H, \quad (1d)$$

where E and ν denote Young's modulus and Poisson's ratio and subscripts p and z stands for porcelain and zirconia. All calculations employ (E_p, E_z) = (70, 210) GPa, (ν_p, ν_z) = (0.20, 0.32).

Initiation of channel cracks in the veneering porcelain is a precondition for delamination growth. This occurs when the tensile stress at the lower surface of porcelain, σ_p, reaches a critical value σ_F. Using standard beam theory calculations for a bilayer, we found

$$\sigma_p=0.75P(l-d)[\underline{q}\,\underline{E}/bH^2][(1-\underline{E})(\underline{q}-\underline{h})^3+(1-\underline{q})^3+\underline{E}\,\underline{q}^3]^{-1} \quad (2a)$$

$$\underline{q}\equiv 0.5[1-\underline{h}^2(1-\underline{E})]/[1-\underline{h}(1-\underline{E})] \quad (2b)$$

3. Results

Figure 2 shows selected frames from three video sequences representing the PFZ (a), PFGZ (b) and PFGGZ (c) groups. Channel cracks initiate from the tensile surface of porcelain and arrest at the veneer/core interface. With increasing load delamination initiate from the tips of these cracks and propagate along the fused interface, generally stably with load. Final failure occurs by fracture of the zirconia core, which usually takes place after the veneer nearly fully delaminates from the core (Fig. 2d). The three material groups differed primarily in the load level at which delamination growth initiates, with minimum for PFZ and maximum for PFGZ.

The interfacial fracture energy G_C is calculated from Eq. 1. In the interest of simplicity the calculations are based on the initial phase of cracking along the interface, $c/s = 0$; as shown in the PFZ study [27], the fracture energy G_C is virtually constant during delamination growth, as is expected from a material property. Accordingly, with $f = 1$ in Eq. 1 one has $G_C = G_{ss}(P = P_i)$, where P_i is the load needed to initiate delamination growth as found from the video footage. The results are given in Fig. 3a, where different symbols represent different test groups. Notwithstanding large experimental scatter, G_C for each group seems insensitive to the veneer thickness. The mean and standard deviation G_C values for the graded zirconia interface are 18.9(3.4) N/m, as compared with 6.2(0.96) N/m for the control PFZ. The data for PFGGZ group (10.2(1.2) N/m) are between these extremes. Fig. 4a shows typical SEM micrographs of the delaminated interfaces for the PFZ and PFGZ groups while Fig 4b is a front view micrograph showing the interface crack in a PFZ specimen after unloading. Fig. 4c is a head-on view of a polished section of the graded zirconia surface. As evident, while the PFZ interface is relatively smooth, the PFGZ interface exhibits a uniform distribution of glass particles on the zirconia bonding surface consistent with the surface morphology in Fig. 4c.

The tensile stress needed to initiate channel cracks in the veneer is calculated from Eq. 2 with P taken as the load at which a channel crack first emerges in the video record. The mean(SD) values for the three material groups are 44(6.2) MPa, which is quite similar to the mean value reported for a free standing porcelain layer [28] or porcelain layer fused onto zirconia [29]. An apparent failure stress value associated with core fracture is found from Eq. 2 assuming that the specimen is a monolith zirconia with thickness $H - h$. The mean(SD) values from all three groups are 698(120) MPa. (It should be noted that these data might not represent a true failure stress of the material due to stress concentration effects associated with cracks in the veneer (e.g., Fig. 2d)).

4. Discussion

The interfacial fracture energy of thin porcelain layer fused onto the graded surface of zirconia core with or without an intermittent residual glass layer is compared with that for unmodified (control) zirconia using the four-point-bending specimen. The fracture sequence consists of unstable growth of channel cracks from the tensile porcelain surface followed by arrest at the veneer/core interface, initiation of delamination from tips of channel cracks, and finally delamination growth along the fused interface. The latter generally occurred stably,

which is due to a stress shielding effect facilitated by adjacent channel cracks [27]. Such geometric enhancement of load bearing capacity is common in film/substrate systems [30,31] as well as canine teeth of wild animals, where the development of channel cracks in the thin enamel coat helps delay fracture into the dentin core [32,33]. The G_C value for the graded zirconia group (PFGZ), here determined at onset of delamination growth where the stress shielding effect is non-existent or minimal, was approximately 3 times that of the control PFZ system. As shown in Fig. 3b this improvement parallels that found in a study of adhesion between a dental composite and sand-blasted zirconia under mode I loading conditions [19], where the use of graded zirconia led to a similar increase in G_C (i.e., from 16 to 43 N/m). In both cases, the effect of sand blasting is small so that the increased resistance to interfacial failure is largely due to the presence of embedded glass phase on the zirconia bonding surface (Fig. 4b). In addition to enhancing adhesion to zirconia, the glass particles in Fig. 4a for PFGZ increase the fracture surface area thus leading to a greater G_C value as seen in Fig. 3a. As shown in Fig. 3a, the existence of a residual glass layer between porcelain and zirconia (group PFGGZ) also increase the interfacial strength, but this increase is quite modest and furthermore it is marred by large scatter.

It is interesting to compare the present G_C values with those for similar PFZ systems obtained elsewhere. Le Thanh [34] reported a value of 12.4 N/m for porcelain veneered to zirconia. Göstemeyer et al. [8] studied VM9, Triceram, Zirox and Lava porcelains veneered zirconia. The reported G_C values for these materials under rapid/slow cooling conditions were 17.1/13.0, 13.3/9.8, 12.8/11.6, and 8.2/7.5 N/m, in that order. The slow-cooling G_C values in these sources well exceed the present value of ≈ 6.2 N/m, which may be partially due to the stress shielding effect noted earlier, the effect that has not been considered in these works. The dependence of G_C on cooling rates in [34] is attributable to the formation of significant residual tensile stresses in the veneer under rapid cooling [10,12–14,16]; such stresses tend to reduce the interfacial energy release rate and thus lead to larger apparent G_C values.

The present benefit afforded by the use of graded zirconia integrates into other mechanical benefits. As shown in ref. [35–37], when using in bilayer or monolithic structures, the lower Young's modulus of the graded zirconia acts to reduce the tensile stress in the graded zone and thus increase the load needed to cause structural failure. Recently, the use of graded zirconia was examined on the structural level in a study of fatigue limits of monolithic zirconia FDPs [38]. Again, the results show a significant improvement in load bearing capacity after the addition of silica and glass onto the zirconia surface. The use of interlayer glass between porcelain and zirconia was also found to reduce delamination areas [39], though in the present work the improvement in G_C was quite modest and furthermore marred by large scatter (Fig. 3a). To gain further insight into the mechanical performance of graded zirconia, we indented graded and ungraded zirconia surfaces with 0.8 mm diameter tungsten carbide ball and observed the contact surface after unloading. While a full report of this work is planned for the future, as shown in Fig. 5 the graded zirconia surface drastically improve the resistance to ring cracking. It is important to note that the determination of critical load for the onset of ring cracks in the graded zirconia surface was not possible since the tungsten carbide indenters all fractured before the initiation of any ring cracking. This remarkable resistance to contact damage is due to the fact that the load needed to initiate

ring cracks is proportional to the surface modulus E, which is much smaller in the graded zirconia surface [40].

As already noted, fracture along the P/Z interface in prosthetic dental crowns and connectors is quite common. Once formed, the delamination crack may graze along the interface, penetrate the core or deflect toward the free surface to form a chip. The specific behavior depends on a wealth of variables including crown geometry, loading conditions, residual stresses and fracture energies of veneer, core and interface. The four-point-bending specimen used here is a mixed-mode type with nearly equal parts of mode I and mode II ERR [24,41]. For general purposes a full mode mix toughness spectrum might be needed.

5. Conclusions

The resistance to delamination growth in modified PFZ systems was determined using the four-point-bending specimen. The interfacial fracture energy G_C of graded zirconia was three times that of the unmodified (control) zirconia (Fig. 3a). Together with a similar increase in the mode I fracture energy G_C of dental composites adhesively bonded to graded zirconia (Fig. 3b), improved resistance to contact damage (Fig. 5) and better esthetics [42], graded zirconia emerges as a viable dental material concept for enhancing mechanical performance, in particular circumventing the low resistance to delamination growth in PFZ systems.

Acknowledgments

This work was sponsored by funding from the United States National Institutes of Health (P.I. Y. Zhang, Grant Nos. R01DE017925, R01DE026772 and R01DE026279), the United States National Science Foundation (P.I. Y. Zhang, Grant No. CMMI-0758530), and the Israeli Science Foundation (P.I. H. Chai, ISF Grant No. 810/09).

References

1. Zarone F, Russo S, Sorrentino R. From porcelain-fused-to-metal to zirconia: Clinical and experimental considerations. Dent Mater. 2011; 27:83–96. [PubMed: 21094996]
2. Ohlmann B, Rammelsberg P, Schmitter M, Schwarz S, Gabbert O. All-ceramic inlay-retained fixed partial dentures: Preliminary results from a clinical study. J Dent. 2008; 36:692–696. [PubMed: 18550253]
3. Liu Y, Liu G, Wang Y, Shen JZ, Feng H. Failure modes and fracture origins of porcelain veneers on bilayer dental crowns. Int J Prosthodont. 2014; 27:147–150. [PubMed: 24596912]
4. Pang Z, Chughtai A, Sailer I, Zhang Y. A fractographic study of clinically retrieved zirconia-ceramic and metal-ceramic fixed dental prostheses. Dent Mater. 2015; 31:1198–1206. [PubMed: 26233469]
5. Aboushelib MN, Feilzer AJ, Kleverlaan CJ. Bridging the gap between clinical failure and laboratory fracture strength tests using a fractographic approach. Dent Mater. 2009; 25:383–391. [PubMed: 18926566]
6. Liu D, Matinlinna JP, Pow EHN. Insights into porcelain to zirconia bonding. J Adhes Sci Technol. 2012; 26:1249–1265.
7. Baldassarri M, Zhang Y, Thompson VP, Rekow ED, Stappert CF. Reliability and failure modes of implant-supported zirconium-oxide fixed dental prostheses related to veneering techniques. J Dent. 2011; 39:489–498. [PubMed: 21557985]
8. Göstemeyer G, Jendras M, Dittmer MP, Bach FW, Stiesch M, Kohorst P. Influence of cooling rate on zirconia/veneer interfacial adhesion. Acta Biomater. 2010; 6:4532–4538. [PubMed: 20601242]
9. Suansuwan N, Swain MV. New approach for evaluating metal-porcelain interfacial bonding. Int J Prosthodont. 1999; 12:547–552. [PubMed: 10815609]

10. Baldassarri M, Stappert CF, Wolff MS, Thompson VP, Zhang Y. Residual stresses in porcelain-veneered zirconia prostheses. Dent Mater. 2012; 28:873–879. [PubMed: 22578663]
11. Hermann I, Bhowmick S, Zhang Y, Lawn BR. Competing fracture modes in brittle materials subject to concentrated cyclic loading in liquid environments: Trilayer structures. J Mater Res. 2006; 21:512–521.
12. Mainjot AK, Schajer GS, Vanheusden AJ, Sadoun MJ. Influence of zirconia framework thickness on residual stress profile in veneering ceramic: Measurement by hole-drilling. Dent Mater. 2012; 28:378–384. [PubMed: 22153718]
13. Meira JB, Reis BR, Tanaka CB, Ballester RY, Cesar PF, Versluis A, Swain MV. Residual stresses in Y-TZP crowns due to changes in the thermal contraction coefficient of veneers. Dent Mater. 2013; 29:594–601. [PubMed: 23561942]
14. Swain MV. Unstable cracking (chipping) of veneering porcelain on all-ceramic dental crowns and fixed partial dentures. Acta Biomater. 2009; 5:1668–1677. [PubMed: 19201268]
15. Fabris D, Souza JC, Silva FS, Fredel M, Mesquita-Guimaraes J, Zhang Y, Henriques B. Thermal residual stresses in bilayered, trilayered and graded dental ceramics. Ceram Int. 2017; 43:3670–3678. [PubMed: 28163345]
16. Tanaka CB, Harisha H, Baldassarri M, Wolff MS, Tong H, Meira JB, Zhang Y. Experimental and finite element study of residual thermal stresses in veneered Y-TZP structures. Ceram Int. 2016; 42:9214–9221. [PubMed: 27087734]
17. Santos RL, Silva FS, Nascimento RM, Souza JC, Motta FV, Carvalho O, Henriques B. Shear bond strength of veneering porcelain to zirconia: Effect of surface treatment by cnc-milling and composite layer deposition on zirconia. J Mech Behav Biomed Mater. 2016; 60:547–556. [PubMed: 27058002]
18. Zhang Y, Kim JW. Graded structures for damage resistant and aesthetic all-ceramic restorations. Dent Mater. 2009; 25:781–790. [PubMed: 19187955]
19. Chai H, Kaizer M, Chughtai A, Tong H, Tanaka C, Zhang Y. On the interfacial fracture resistance of resin-bonded zirconia and glass-infiltrated graded zirconia. Dent Mater. 2015; 31:1304–1311. [PubMed: 26365987]
20. Aboushelib MN, Kleverlaan CJ, Feilzer AJ. Microtensile bond strength of different components of core veneered all-ceramic restorations. Part II: Zirconia veneering ceramics. Dent Mater. 2006; 22:857–863. [PubMed: 16376981]
21. Dündar M, Özcan M, Gökçe B, Çömlekoglu E, Leite F, Valandro LF. Comparison of two bond strength testing methodologies for bilayered all-ceramics. Dent Mater. 2007; 23:630–636. [PubMed: 16844212]
22. Fischer J, Stawarzcyk B, Trottmann A, Hammerle CH. Impact of thermal misfit on shear strength of veneering ceramic/zirconia composites. Dent Mater. 2009; 25:419–423. [PubMed: 18990436]
23. Guess PC, Kulis A, Witkowski S, Wolkewitz M, Zhang Y, Strub JR. Shear bond strengths between different zirconia cores and veneering ceramics and their susceptibility to thermocycling. Dent Mater. 2008; 24:1556–1567. [PubMed: 18466964]
24. Charalambides PG, Cao HC, Lund J, Evans AG. Development of a test method for measuring the mixed mode fracture resistance of bimaterial interfaces. Mech Mater. 1990; 8:269–283.
25. Tholey MJ, Waddell JN, Swain MV. Influence of the bonder on the adhesion of porcelain to machined titanium as determined by the strain energy release rate. Dent Mater. 2007; 23:822–828. [PubMed: 16908059]
26. Chai H, Fox J. On delamination growth from channel cracks in thin-film coatings. Int J Solids Struct. 2012; 49:3142–3147.
27. Chai H, Lee JJ, Mieleszko AJ, Chu SJ, Zhang Y. On the interfacial fracture of porcelain/zirconia and graded zirconia dental structures. Acta Biomater. 2014; 10:3756–3761. [PubMed: 24769152]
28. Meyer JM, O'Brien WJ, Yu CU. Sintering of dental porcelain enamels. J Dent Res. 1976; 55:696–699. [PubMed: 1064616]
29. White SN, Miklus VG, McLaren EA, Lang LA, Caputo AA. Flexural strength of a layered zirconia and porcelain dental all-ceramic system. J Prosthodont Dent. 2005; 94:125–131.
30. Chai H. Channel cracking in inelastic film/substrate systems. Int J Solids Struct. 2011; 48:1092–1100.

31. Thouless MD, Olsson E, Gupta A. Cracking of brittle films on elastic substrates. Acta Metall Mater. 1992; 40:1287–1292.
32. Freeman PW, Lemen C. An experimental approach to modeling the strength of canine teeth. J Zool. 2007; 271:162–169.
33. Lawn BR, Chai H, Barani A, Bush MB. Transverse fracture of canine teeth. J Biomech. 2013; 46:1561–1567. [PubMed: 23623329]
34. Le Thanh, R. Adhesion of veneering porcelain to zirconium dioxide ceramic as determined by the strain energy release rate. Sydney, Australia: The University of Sydney; 2009.
35. Zhang Y, Chai H, Lawn BR. Graded structures for all-ceramic restorations. J Dent Res. 2010; 89:417–421. [PubMed: 20200413]
36. Villefort RF, Amaral M, Pereira GK, Campos TM, Zhang Y, Bottino MA, Valandro LF, de Melo RM. Effects of two grading techniques of zirconia material on the fatigue limit of full-contour 3-unit fixed dental prostheses. Dent Mater. 2017; 33:e155–e164. [PubMed: 28118929]
37. Zhang Y, Ma L. Optimization of ceramic strength using elastic gradients. Acta Mater. 2009; 57:2721–2729. [PubMed: 20161019]
38. Zhang Y, Sun MJ, Zhang DS. Designing functionally graded materials with superior load-bearing properties. Acta Biomater. 2012; 8:1101–1108. [PubMed: 22178651]
39. Passos SP, Linke B, Major PW, Nychka JA. Improving the compatibility of an Y-TZP/porcelain system using, a new composite interlayer composition. J Mech Behav Biomed Mater. 2017; 65:11–19. [PubMed: 27544615]
40. Kim JW, Liu L, Zhang Y. Improving the resistance to sliding contact damage of zirconia using elastic gradients. J Biomed Mater Res B. 2010; 94:347–352.
41. Mei HX, Pang YY, Huang R. Influence of interfacial delamination on channel cracking of elastic thin films. Int J Fract. 2007; 148:331–342.
42. Ren L, Janal MN, Zhang Y. Sliding contact fatigue of graded zirconia with external esthetic glass. J Dent Res. 2011; 90:1116–1121. [PubMed: 21666105]
43. Zhang Y, Kim JW. Graded zirconia glass for resistance to veneer fracture. J Dent Res. 2010; 89:1057–1062. [PubMed: 20651092]

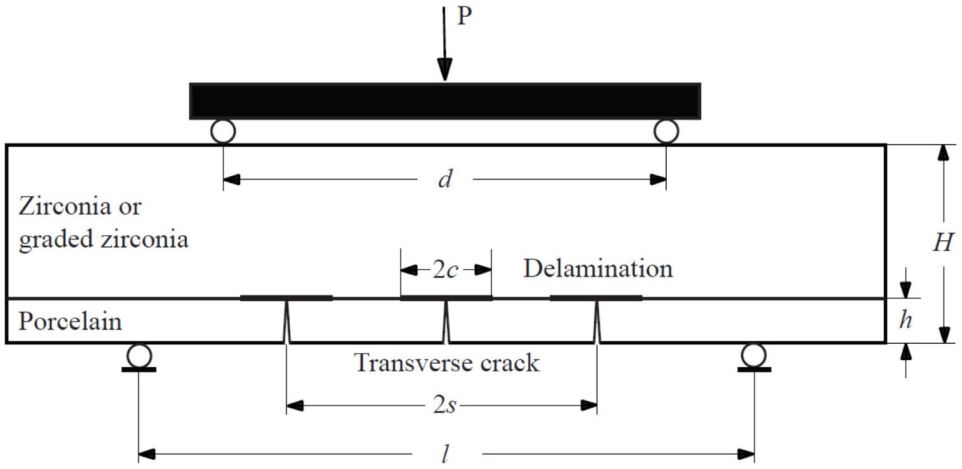

Figure 1.

The four-point-bending apparatus used to determine the interfacial fracture energy of porcelain fused to zirconia or graded zirconia. The fracture model shown is based on *in situ* observations. In this work, the calculation of interfacial fracture energy G_C is limited to the onset of delamination growth ($c = 0$), as determined from the video footage.

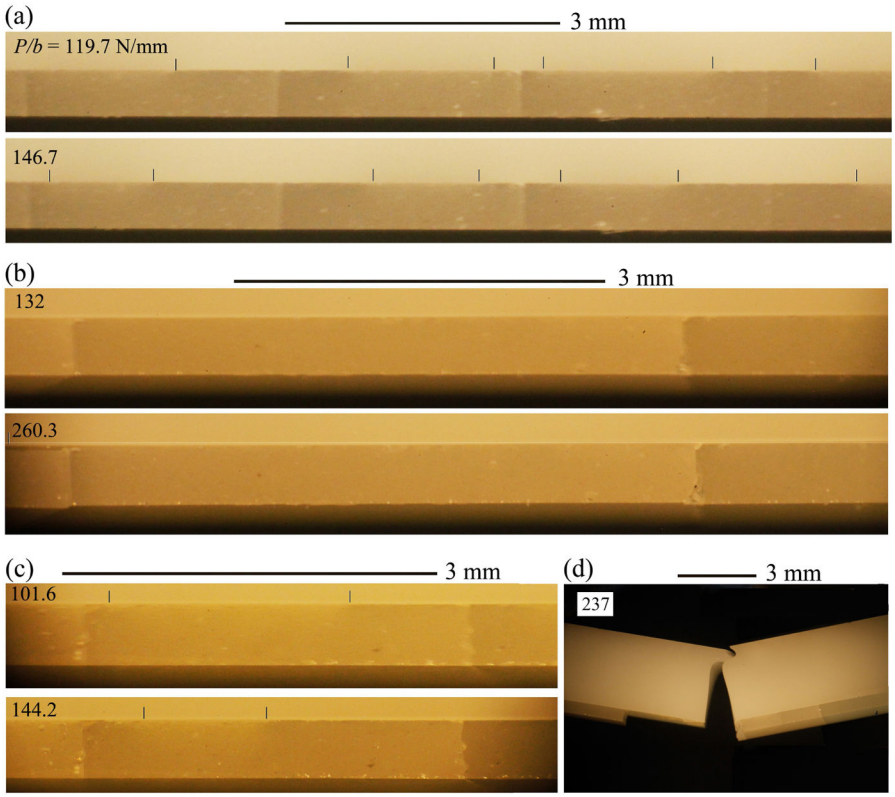

Figure 2.

Selected frames from three video sequences for: (a) control porcelain/zirconia (PFZ), (b) porcelain/graded zirconia (PFGZ), (c) porcelain/graded zirconia with an intermittent glass layer (PFGGZ). In each case, the failure sequence is represented by two frames, identified by applied force per unit beam width *P/b*. After the formation of vertical channel cracks in porcelain, delamination initiated and propagated from the tips of these cracks (small vertical lines). (d) Complete fracture of the PFGGZ bilayer in (c).

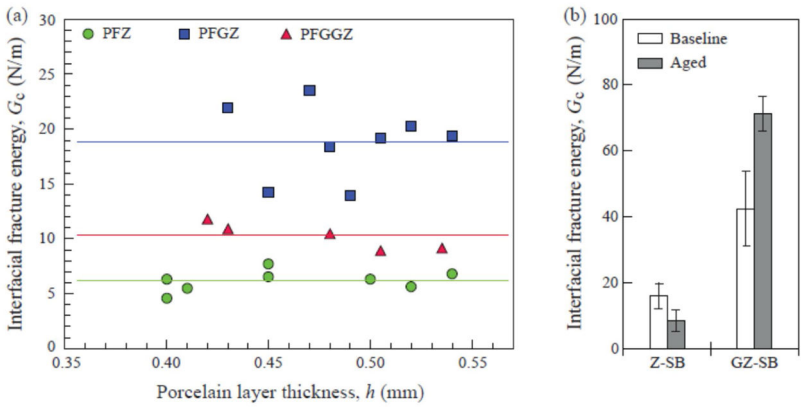

Figure 3.

(a) Interfacial fracture energy G_C vs. porcelain layer thickness h for the three material systems studied; solid lines are mean values. (b) Mode I fracture energy for adhesion failure between a dental composite and graded (GZ) or ungraded (Z), sandblasted (SB) zirconia surfaces, as obtained using the wedge-loaded double cantilever beam (WDCB) test specimen [19]. As shown, the use of graded zirconia greatly increased G_C for both baseline (tested within a week after cementation) and aged (subjected to 20,000 thermal cycles between 5 °C and 55 °C and 60 days incubation at 37 °C in water) conditions.

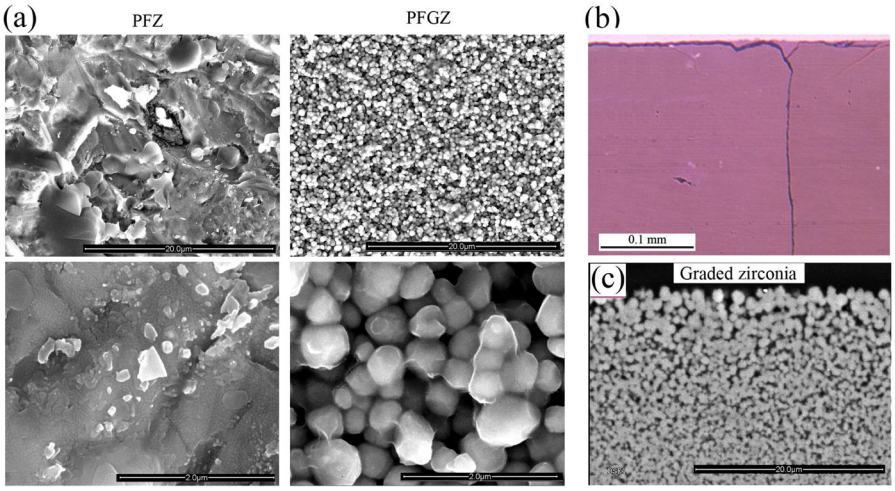

Figure 4.

(a) Typical SEM micrographs of the delaminated surface for PFZ (left) and PFGZ (right). The surface for the graded zirconia (right side) is relatively rough, consistent with a greater fracture energy G_C. (b) A front view micrograph in a PFZ specimen taken after unloading, showing how a crack in porcelain branches into the P/Z interface. (c) Morphology of the graded zirconia showing a high glass content close to the free surface [43].

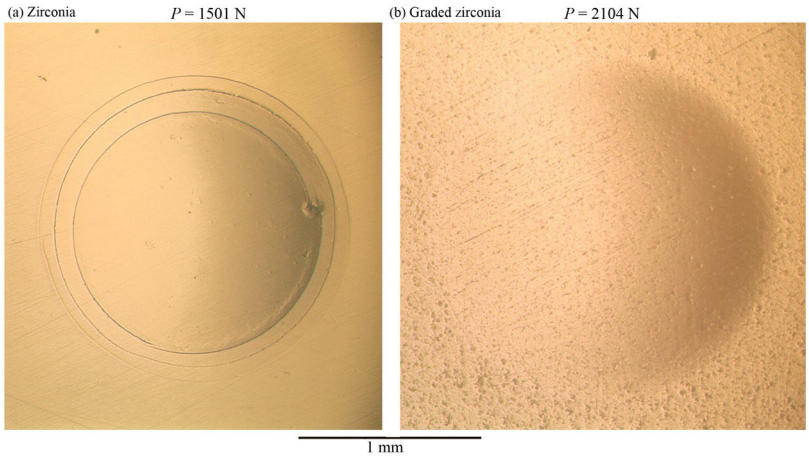

Figure 5.

Two micrographs from our preliminary study demonstrating the mechanical advantage of graded zirconia under indentation loading. The images correspond to indentation with 0.8 mm diameter tungsten carbide ball of (a) zirconia and (b) graded zirconia surfaces. Although loaded by a greater force *(P* = 2104 N vs. 1501 N), the graded zirconia surface is intact while the unmodified zirconia surface exhibits numerous ring cracks outside the contact circle.